Heat transport properties within living biological tissues with temperature-dependent thermal properties

Ying-Ze Wang(王颖泽)[†], Xiao-Yu Lu(陆晓宇), and Dong Liu(刘栋)

Department of Energy and Power Engineering, Jiangsu University, Zhenjiang 212013, *China*

(Received 11 March 2022; revised manuscript received 5 April 2022; accepted manuscript online 28 April 2022)

Understanding of the heat transport within living biological tissues is crucial to effective heat treatments. The heat transport properties of living biological tissues with temperature-dependent properties are explored in this paper. Taking into account of variable physical properties, the governing equation of temperature is first derived in the context of the dual-phase-lags model (DPL). An effective method, according to the Laplace transform and a linearization technique, is then employed to solve this nonlinear governing equation. The temperature distribution of a biological tissue exposed to a pulsed heat flux on its exterior boundary, which frequently happens in various heat treatments, is predicted and analyzed. The results state that a lower temperature can be predicted when temperature dependence is considered in the heating process. The contributions of key thermal parameters are different and dependent on the ratio of phase lag and the amplitude of the exterior pulsed heat flux.

Keywords: bio-heat transfer, biological tissue, temperature dependence, analytical procedure

PACS: 44.10.+i, 87.55.dh **DOI:** 10.1088/1674-1056/ac6b29

1. Introduction

With the development of many techniques like microwave, laser and ultrasound, various thermal therapies to cure diseased and injured skin tissue, such as hyperthermia, cryosurgery, cryopreservation for skin cancer and skin burns, are widely used in clinic trails. Understanding of the primary mechanism behind these therapies and further monitoring of the temperature distribution are both crucial to optimizing the thermal dose and expanding its popularization of clinical application.[1–5]

The temperature distribution of biological tissues can be attributed to heat transfer coupled with the complicated physiological process.[2,6] This physical process can be described by an effective mathematical model of bio-heat transfer, and then the thermal dose fitting the clinic outcomes can be calculated on this basis. A famous model of bio-heat transfer, proposed by Pennes on the classical Fourier's law,[7] is widely used to explore the heat transport properties within living biological bodies. Considering its non-homogeneous inner structure, non-Fourier heat conduction behavior like wave-like distribution of temperature absent in the Pennes model, has been observed in some experiments.[8,9] To explain this non-Fourier effect, some modified models constructed in the relaxation mechanism, including the CV or named TW model,[10,11] the DPL model,[12] and the generalized DPL model,[13] have been introduced successively to explore the heat transport properties within living biological tissues.[14–20]

Notwithstanding lots of results on thermal response occurring in living biological tissues have been obtained, a constant property hypothesis is employed in these studies for simplicity of solution.[14–20] However, the physical properties of biological tissues are temperature-dependent in general, and this temperature dependence will affect the final temperature response. Consequently, for the effective prediction of temperature distribution, these temperature-dependent thermal parameters should be considered. The dependence of the blood perfusion rate on temperature has been analyzed in the work of Zhang *et al.*, showing that an evident temperature change will happen for variations of quadratic blood perfusion rate.[21] Kumar *et al.*[22] and Arefmanesh *et al.*[23] discussed the heat transport involving variable thermal properties and pointed out that modified DPL model with temperature-dependent terms is the closest to the experimental results. Considering the coupled thermo-mechanical effect, Wang *et al.* further explored the effect of variable blood perfusion with temperature on thermo-mechanical coupled behavior.[24] Furthermore, the detailed parametric study has been constructed by Guntur *et al.*[25] and Guntur and Choi[26] stated that a lower temperature will be predicted by the change of thermal properties when the tissue is heated.

This work explores the effect of temperature-dependent thermal parameters on heat transport properties in living biological tissues. Owing to the function of parameters varying with temperature, a non-linear governing equation with variable physical properties is proposed through DPL model. The non-linear terms are discretized by a linearization technique, and the approximate analytical solution is derived by the Laplace transform and its limit theorem. The temperature response of a skin tissue exposed to a boundary pulsed heat flux is predicted. Comparison with the results from the

[†]Corresponding author. E-mail: wyz3701320@ujs.edu.cn

© 2023 Chinese Physical Society and IOP Publishing Ltd

constant properties is also performed to evaluate the effect of temperature dependence.

2. Formulation of problem

The general bio-heat transfer equation, proposed by Pennes,[7] is given as follows:

$$\rho c\frac{\partial T}{\partial t}=k\nabla^2 T+w_{\rm b}\rho_{\rm b}c_{\rm b}\left(T_{\rm b}-T\right)+q_{\rm met}+q_{\rm ext}, \tag{1}$$

in which T is the tissue temperature, $T_{\rm b}$ is the blood temperature, k is the tissue thermal conductivity, ρ, c and $\rho_{\rm b}$, $c_{\rm b}$ are the mass density and specific heat of tissue and blood separately, $w_{\rm b}$ is the blood perfusion rate, $q_{\rm met}$ is the metabolic heat generation, and $q_{\rm ext}$ is the volumetric heating.

Note that a nonphysical assumption with infinite speed of heat transport is involved in Pennes model. To overcome this drawback of the Pennes model, some modified model rooted in different phase lag mechanisms are employed to depict the heat transport occurring in biological tissues.[10–13]

Admitting a delay to exist in the heat transport within biological tissues due to its non-homogeneous inner structure, the DPL bio-heat equation can be taken as

$$\begin{aligned}&\left(1+\tau_q\frac{\partial}{\partial t}\right)\left[\rho c\frac{\partial T}{\partial t}-w_{\rm b}\rho_{\rm b}c_{\rm b}\left(T_{\rm b}-T\right)\right]\\&=k\left(1+\tau_T\frac{\partial}{\partial t}\right)\nabla^2 T+\left(1+\tau_q\frac{\partial}{\partial t}\right)\left(q_{\rm met}+q_{\rm ext}\right),\end{aligned} \tag{2}$$

where τ_q and τ_T are the phase lags defined by Tzou to describe the effect of thermal inertia (temporal effect) and microstructure interaction (spatial effect).

Considering that these thermal physical parameters included in Eq. (2) are temperature dependent, that is, $\{k,c,\alpha,\rho,w_{\rm b}\}=\{k(T),c(T),\alpha(T),\rho(T),w_{\rm b}(T)\}$, equation (2) should be rewritten as

$$\begin{aligned}&\left(1+\tau_q\frac{\partial}{\partial t}\right)\left[\rho(T)c(T)\frac{\partial T}{\partial t}-w_{\rm b}(T)\rho_{\rm b}c_{\rm b}\left(T_{\rm b}-T\right)\right]\\&+\tau_q\left\{\frac{\partial}{\partial t}\left[\rho(T)c(T)\right]\frac{\partial T}{\partial t}-\rho_{\rm b}c_{\rm b}\left(T_{\rm b}-T\right)\frac{\partial w_{\rm b}(T)}{\partial t}\right\}\\&=\nabla\left[k(T)\left(1+\tau_T\frac{\partial}{\partial t}\right)\nabla T\right]+\left(1+\tau_q\frac{\partial}{\partial t}\right)\left(q_{\rm met}+q_{\rm ext}\right).\end{aligned} \tag{3}$$

Now, we come to consider the one-dimensional (1D) bio-heat transfer problem that a biological tissue exposed to a pulsed heat flux on its exterior surface, which frequently happens in heat treatments. As depicted in Fig. 1, the thickness of the region occupied by this biological tissue is L. On the upper boundary there is a transient heat flux at time $t>0$, while its bottom boundary is treated as being thermally insulated. The initial temperature is taken as the uniform temperature T_0.

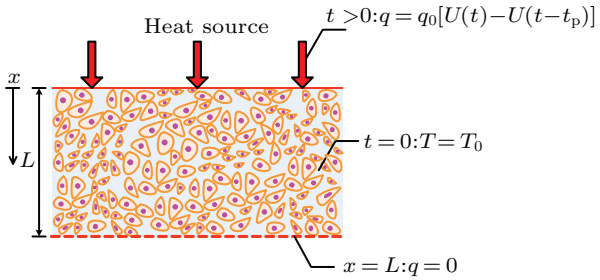


Fig. 1. Schematic view of biological tissue.

Let the x-coordinate be parallel to the thickness direction of the skin tissue, then the 1D forms of Eq. (3) with temperature-dependent thermal parameters will be rewritten as

$$\begin{aligned}&\left(1+\tau_q\frac{\partial}{\partial t}\right)\left[\rho(T)c(T)\frac{\partial T}{\partial t}-w_{\rm b}(T)\rho_{\rm b}c_{\rm b}\left(T_{\rm b}-T\right)\right]\\&+\tau_q\left\{\frac{\partial}{\partial t}\left[\rho(T)c(T)\right]\frac{\partial T}{\partial t}-\rho_{\rm b}c_{\rm b}\left(T_{\rm b}-T\right)\frac{\partial w_{\rm b}(T)}{\partial t}\right\}\\&=\frac{\partial}{\partial x}\left[k(T)\left(1+\tau_T\frac{\partial}{\partial t}\right)\frac{\partial T}{\partial x}\right]\\&+\left(1+\tau_q\frac{\partial}{\partial t}\right)\left(q_{\rm met}+q_{\rm ext}\right).\end{aligned} \tag{4}$$

The initial and boundary conditions are assumed to be in the following forms:

$$T(x,0)=T_0,\quad \frac{\partial T(x,0)}{\partial t}=0, \tag{5}$$

$$q(0,t)=q_0\left[U(t)-U(t-t_p)\right],\quad q(L,t)=0. \tag{6}$$

Some dimensionless variables are introduced to normalize the governing equation (4) below:

$$\begin{aligned}&x^*=\sqrt{\frac{h_{\rm b}(T_0)}{k(T_0)}}x,\quad t^*=\frac{h_{\rm b}(T_0)}{\rho(T_0)c(T_0)}t,\\&\left(\tau_q^*,\tau_T^*,t_p^*\right)=\frac{h_{\rm b}(T_0)}{\rho(T_0)c(T_0)}\left(\tau_q,\tau_T,t_p\right),\\&T^*=\frac{T(x^*t^*)-T_0}{q_0}\sqrt{k(T_0)h_{\rm b}(T_0)},\\&L^*=\sqrt{\frac{h_{\rm b}(T_0)}{k(T_0)}}L,\quad\text{and}\quad q_i^*=\sqrt{\frac{k(T_0)}{h_{\rm b}(T_0)}}\frac{q_i}{q_0}\end{aligned}$$

in which $h_{\rm b}(T_0)=w_{\rm b}(T_0)\rho_{\rm b}c_{\rm b}$.

Substituting these dimensionless variables into Eq. (4) and removing the asterisks of each dimensionless variable for convenience, we have

$$\begin{aligned}&\left(1+\tau_q\frac{\partial}{\partial t}\right)\left[f_{\rho(T)}f_{c(T)}\frac{\partial T}{\partial t}-f_{w_{\rm b}(T)}\left(T_{\rm b}-T\right)\right]\\&+\tau_q\left\{\frac{\partial f_{\rho(T)}f_{c(T)}}{\partial t}\frac{\partial T}{\partial t}-\left(T_{\rm b}-T\right)\frac{\partial f_{w_{\rm b}(T)}}{\partial t}\right\}\\&=f_{k(T)}\left(1+\tau_T\frac{\partial}{\partial t}\right)\frac{\partial^2 T}{\partial x}+\frac{\partial f_{k(T)}}{\partial x}\left(1+\tau_T\frac{\partial}{\partial t}\right)\frac{\partial T}{\partial x}\\&+\left(1+\tau_q\frac{\partial}{\partial t}\right)\left(q_{\rm met}+q_{\rm ext}\right),\end{aligned} \tag{7}$$

in which $f_{p(T)} = P(T)/P(T_0)$ is non-dimensional ratio of P at temperature T' to that at T_0, where P represents all temperature-dependent variable physical parameters.

The initial and boundary conditions in the dimensionless form can be expressed as

$$T(x,0) = 0, \quad \frac{\partial T(x,0)}{\partial t} = 0, \tag{8}$$

$$\begin{aligned} & f_{k(T)}\left(1+\tau_T\frac{\partial}{\partial t}\right)\frac{\partial T}{\partial x} \\ = & \left(1+\tau_q\frac{\partial}{\partial t}\right)\left\{U\left[\frac{\rho(T_0)c(T_0)}{h_{\mathrm{b}}(T_0)}(t-t_p)\right]\right. \\ & \left.-U\left[\frac{\rho(T_0)c(T_0)}{h_{\mathrm{b}}(T_0)}t\right]\right\}, \end{aligned} \tag{9}$$

$$\left(1+\tau_T\frac{\partial}{\partial t}\right)\frac{\partial T}{\partial x} = 0. \tag{10}$$

3. Solution of problems

3.1. Linearization of governing equations

It is obvious that the governing equation (7) is nonlinear when these temperature-dependent thermal parameters are considered, which makes an analytical solution practically impossible. Therefore, some linearizing techniques should be applied to this nonlinear equation. Here, a layer method is employed to disperse these temperature-dependent parameters $\left\{f_{\rho(T)}, f_{\mathrm{c}(T)}, f_{w_{\mathrm{b}}(T)}, f_{k(T)}\right\}$. As shown in Fig. 2, the initial skin structure is replaced by a new n-layered substructure, in which the thickness of each layer is $\Delta x = L/n$. Owing to the linear layer mechanism that any continuous curve can be closely approximated by a series of straight lines, the continues temperature $T(x,t)$ can be dispersed discretized into $T^i(x,t)$ $(i = 1,2,\ldots,n)$ for a given time t, which means the temperature $T^i(x,t)$ is uniform in each layer but varies from one layer to another. Consequently, the temperature-dependent parameters $\left\{f_{\rho(T)}, f_{\mathrm{c}(T)}, f_{w_{\mathrm{b}}(T)}, f_{k(T)}\right\}$ can be replaced by $\left\{f_{\rho(T^i)}, f_{\mathrm{c}(T^i)}, f_{w_{\mathrm{b}}(T^i)}, f_{k(T^i)}\right\}$ in the discrete forms.

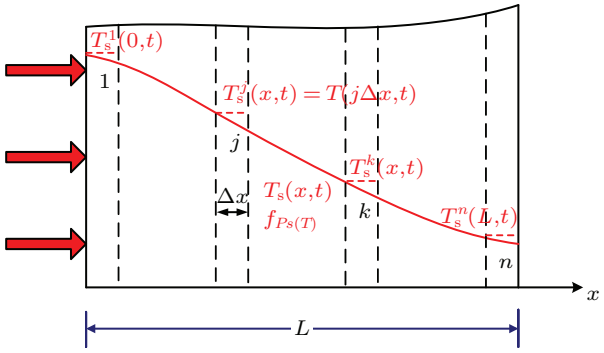


Fig. 2. The n-layered structure with distinct material properties.

Utilizing these linearized treatments, equation (7) can be linearized as

$$\begin{aligned} & \left(1+\tau_q\frac{\partial}{\partial t}\right)\left[f_\rho^i f_{\mathrm{c}}^i\frac{\partial T^i}{\partial t} - f_{w_{\mathrm{b}}}^i\left(T_{\mathrm{b}} - T^i\right)\right] \\ = & f_k^i\left(1+\tau_T\frac{\partial}{\partial t}\right)\frac{\partial^2 T^i}{\partial x} + \left(1+\tau_q\frac{\partial}{\partial t}\right)q_{\mathrm{met}}^i, \end{aligned} \tag{11}$$

where

$$\left\{f_\rho^i, f_{\mathrm{c}}^i, f_{w_{\mathrm{b}}}^i, f_k^i\right\} = \left\{f_{\rho(T^i)}, f_{\mathrm{c}(T^i)}, f_{w_{\mathrm{b}}(T^i)}, f_{k(T^i)}\right\}.$$

Equations (8)–(10) with layered forms take the following forms:

$$T^i = 0, \quad \frac{\partial T^i}{\partial t} = 0, \quad (i = 1,2,\ldots,n), \tag{12}$$

$$\begin{aligned} & f_k^1\left(1+\tau_T\frac{\partial}{\partial t}\right)\frac{\partial T^1}{\partial x} \\ = & \left(1+\tau_q\frac{\partial}{\partial t}\right)\left\{U\left[\frac{\rho(T_0)c(T_0)}{h_{\mathrm{b}}(T_0)}(t-t_p)\right]\right. \\ & \left.-U\left[\frac{\rho(T_0)c(T_0)}{h_{\mathrm{b}}(T_0)}t\right]\right\}, \end{aligned} \tag{13}$$

$$\left(1+\tau_T\frac{\partial}{\partial t}\right)\frac{\partial T^n}{\partial x} = 0. \tag{14}$$

Meanwhile, the interior continuous condition satisfying the Kapitza thermal interface model is introduced into the following solutions:[27]

$$X^i q^i = T^i - T^{i+1}, \quad q^i = q^{i+1}, \quad (i = 1,2,\ldots,n-1), \tag{15}$$

in which X^i is a non-negative constant and its limiting cases $X^i = 0$ and $X^i \to \infty$ correspond to the perfectly conductive and thermally insulated interface, respectively.

3.2. Asymptotic solutions of linear governing equations

Applying a Laplace transform to both sides of linearized Eq. (11) and combining the homogeneous initial condition (12) result in

$$\frac{\mathrm{d}^2\bar{T}^i}{\mathrm{d}x^2} - \lambda^i(s)\bar{T}^i = -\beta^i(s)\left[q_{\mathrm{met}}^i + (1+\tau_q s)f_{w_{\mathrm{b}}}^i T_{\mathrm{b}}\right], \tag{16}$$

where

$$\lambda^i(s) = \frac{(1+\tau_q s)\left(f_\rho^i f_{\mathrm{c}}^i s + f_{w_{\mathrm{b}}}^i\right)}{f_k^i(1+\tau_T s)}, \quad \beta^i(s) = \frac{1}{f_k^i(1+\tau_T s)s}.$$

The Laplace transform of the boundary conditions (13) and (14) can be written as

$$\begin{aligned} & \frac{\mathrm{d}\bar{T}^1(0,s)}{\mathrm{d}x} = -\frac{1+\tau_q s}{f_k^1(1+\tau_T s)}\frac{1-\exp(-t_p s)}{s}, \\ & \frac{\mathrm{d}\bar{T}^n(L,s)}{\mathrm{d}x} = 0. \end{aligned} \tag{17}$$

The general solution of Eq. (11) under boundary conditions (17) and a perfectly conductive interface condition (15) $(X^i = 0)$ can be derived as

$$\bar{T}^i\left(x^i,s\right) = \left[1-\exp(-t_p s)\right]\frac{1+\tau_q s}{f_k^1(1+\tau_T s)}\frac{1}{s\sqrt{\lambda^i(s)}}$$

$$\times \frac{\exp\left[\sqrt{\lambda^i(s)}\left(x^i-2L\right)\right]+\exp\left(-\sqrt{\lambda^i(s)}x^i\right)}{1-\exp\left(-2\sqrt{\lambda^i(s)}L\right)} + \frac{q^i_{\rm met}+(1+\tau_q s)f^i_{w_{\rm b}}T_{\rm b}}{\mu^i(s)}, \tag{18}$$

where $\mu^i(s)=\lambda^i(s)/\beta^i(s)$.

Although the analytical solution of $\bar{T}^i(x,t)$ is obtained in the Laplace transform domain, however, complicated $\lambda^i(s)$ leads the direct inverse transform of $\bar{T}^i(x,t)$ to be hardly to perform. Here an approximation of $\lambda^i(s)$, based on the limit theorem of Laplace transform,[28,29,33] is applied to the further solution, which takes the following form:

$$\lambda^i(s)\big|_{s\to\infty}=\frac{\tau_q}{\tau_T}\left(\frac{1}{f^i_\alpha}s+\frac{f^i_{w_{\rm b}}}{f^i_k}\right), \tag{19}$$

where $f^i_\alpha=f^i_k/\left(f^i_\rho f^i_{\rm c}\right)$.

Substituting this approximation into general solution (18) and considering the displacement property and the delay property of Laplace transform, which takes the following form:

$$L^{-1}\left[\bar{f}(s-a)\right]=\exp(at)f(t), \tag{20}$$

$$L^{-1}\left[\exp(-\tau s)\bar{f}(s)\right]=\begin{cases}0, & \text{for } t<\tau,\\ f(t-\tau), & \text{for } t\geq\tau.\end{cases} \tag{21}$$

Then the inverse Laplace transform of $\bar{T}^i\left(x^i,s\right)$ in the time domain can be derived as

$$T^i(x,t)=\begin{cases}T^i_1(x,t)-T^i_1(x,t-t_P)+T^i_2(x,t), & t>t_p,\\ T^i_1(x,t)+T^i_2(x,t), & t\leq t_p,\end{cases} \tag{22}$$

in which

$$\begin{aligned}T^i_1(x,t) =& \frac{\sqrt{f^i_\alpha}}{f^1_k}\sqrt{\frac{\tau_q}{\tau_T}}\exp\left(-\frac{f^i_{w_{\rm b}}}{f^i_\rho f^i_{\rm c}}t\right)\\ &\times\sum_{n=0}^{\infty}\left\{2\sqrt{\frac{t}{\pi}}\exp\left(-\frac{\left[2(n+1)L-x^i\right]^2\frac{\tau_q}{\tau_T}\frac{1}{f^i_\alpha}}{4t}\right)\right.\\ &-\left[2(n+1)L-x^i\right]\sqrt{\frac{\tau_q}{\tau_T}}\sqrt{\frac{1}{f^i_\alpha}}\\ &\times\operatorname{erfc}\left(\frac{\left[2(n+1)L-x^i\right]\sqrt{\frac{\tau_q}{\tau_T}}\sqrt{\frac{1}{f^i_\alpha}}}{2\sqrt{t}}\right)\\ &+2\sqrt{\frac{t}{\pi}}\exp\left(-\frac{(2nL+x_j)^2\frac{\tau_q}{\tau_T}\frac{1}{f^i_\alpha}}{4t}\right)\\ &-(2nL+x_j)\sqrt{\frac{\tau_q}{\tau_T}}\sqrt{\frac{1}{f^i_\alpha}}\\ &\left.\times\operatorname{erfc}\left(\frac{(2nL+x_j)\sqrt{\frac{\tau_q}{\tau_T}}\sqrt{\frac{1}{f^i_\alpha}}}{2\sqrt{t}}\right)\right\},\end{aligned} \tag{23}$$

$$\begin{aligned}T^i_2(x,t) =& \left\{\frac{1}{f^i_{w_{\rm b}}}\left[1-\exp\left(-\frac{f^i_{w_{\rm b}}}{f^i_\rho f^i_{\rm c}}t\right)\right]+\frac{1}{f^i_{w_{\rm b}}-f^i_\rho f^i_{\rm c}/\tau_q}\right.\\ &\left.\times\left[\exp\left(-\frac{f^i_{w_{\rm b}}}{f^i_\rho f^i_{\rm c}}t\right)-\exp\left(-\frac{t}{\tau_q}\right)\right]\right\}q^i_{\rm met}\\ &+\left[1-\exp\left(-\frac{f^i_{w_{\rm b}}}{f^i_\rho f^i_{\rm c}}t\right)\right]T_{\rm b}.\end{aligned} \tag{24}$$

4. Solution of problems

4.1. Verification of solutions

It is necessary to validate the present analytical method for the following evaluation of heat transport properties via explicit solution (22). Since no adequate experimental data are available and similar theoretical results are lacking, direct numerical validation is hard to construct. However, the results with constant properties have been obtained in the present research by using various bio-heat transfer models,[31,32] and those became good samples for the verification of our results. Assume temperature-dependent parameters $\left\{f^i_\rho, f^i_{\rm c}, f^i_{w_{\rm b}}, f^i_k\right\}\equiv 1$, then the solution (22) will be reduced to the case with constant properties. Here the same calculation parameters used in the samples[31,32] are introduced as follows: $k=0.628$ W/(m·K), $\rho=1000$ kg/m^3, $c=4187$ J/(kg·K), $\rho_{\rm b}=1000$ kg/m^3, $c_{\rm b}=4187$ J/(kg·K), $w_{\rm b}=1.87\times10^{-3}$ s^{-1}, $T_{\rm b}=37$ °C, $T_0=37$ °C, $L=5$ cm, $q_{\rm met}=1.19\times10^3$ W/m^3, and $q_0=19\times10^3$ W/m^2.

The dimensionless temperature responses at a skin surface induced by pulsed heat flux with duration time $t_p=3$ s for different bio-heat transfer models are depicted in Fig. 3. Obviously. set $\tau_q=\tau_T$, then the dual-phase-lag equation will be reduced to the Fourier's equation,indicating that the DPL model of bio-heat transfer is identical with the Pennes model. This means that the results predicted by solution (22) should be the same as those predicted by Pennes model, which is confirmed by the temperature distributions illustrated in Fig. 3.

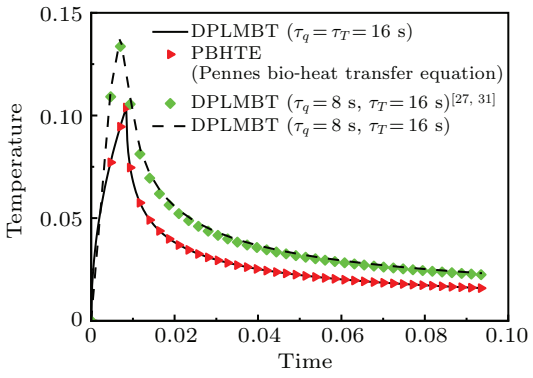


Fig. 3. Plots of time-dependent temperature response at pulsed heat flux surface, predicted by different models of bio-heat transfer.

4.2. Analysis of thermal response

The details of variable physical properties for biological tissues can be obtained from effective experimental data. The effective information about the key thermal parameters with respect to temperature has been obtained by Gun-

tur *et al.*[25] and Guntur and Choi,[26] and the temperature-dependent characteristic curve can be be obtained from the following equation:[26]

$$P(T)=\begin{cases} A_{1o}(T-T_o)^{m_1}+B, & T_1\le T\le T_o,\\ A_{o2}(T-T_o)^{m_2}+B, & T_o\le T\le T_2, \end{cases} \tag{25}$$

in which T_1 and T_2 are the minimum temperature and maximum temperature measured experimentally in the *ex vivo* liver tissue, T_o is the turning temperature, and $B=P(T_o)$, A_{1o} and m_1 are the coefficients best fitting to the measured data for $T_1\le T\le T_o$, while A_{o2} and m_2 are the coefficients best fitting to the measured data for $T_o\le T\le T_2$. These detailed empirical parameters are listed in Table 1.

Meanwhile for evaluating the effect of temperature-dependent blood perfusion rate $w_b(T)$, the linear relation with temperature, frequently used in previous literature, is given as follows:[21]

$$w_b(T)=w_{b0}(1+a_1T), \tag{26}$$

in which a_1 is the empirical coefficient of the linear temperature dependency.

Table 1. Values of empirical parameters of each thermal parameter with temperature measured for *ex vivo* liver tissue.[26]

Thermal parameter	B	T_o (°C)	A_{1o}	A_{o2}	m_1	m_2
Specific heat capacity (J/m^3·K)	3.567×10^6	35	1.10×10^3	5.41×10^2	1.698	1.823
Thermal conductivity (W/m·K)	0.520	35	3.41×10^{-4}	2.70×10^{-4}	1.725	1.642
Thermal diffusivity (m^2/s)	1.41×10^{-7}	35	7.25×10^{-11}	8.06×10^{-12}	1.615	2.151

Based on the physical meaning of DPL model, two relationships for different values of τ_q and τ_T are derived for their cause-and-effect between heat flux and temperature gradient. One is named the gradient relationship for the case $\tau_q>\tau_T$ ($\tau_q/\tau_T>1$), and the other is temperature relationship for the $\tau_q<\tau_T$ ($\tau_q/\tau_T<1$). Although the values of these phase lags are hard to estimate for biological tissues,[13] we also observe that the value of the phase lag τ_q is always larger than that of τ_T or close to each other based on existing experiments and studies,[6,13] which means the gradient precedence dominates the heat transport in biological tissue. As a result, the cases for $\tau_q/\tau_T=8,4,2,1$ are used to implement the following investigation, and the results in the case $\tau_q/\tau_T=1$ are equal to the results predicted by the Pennes model.

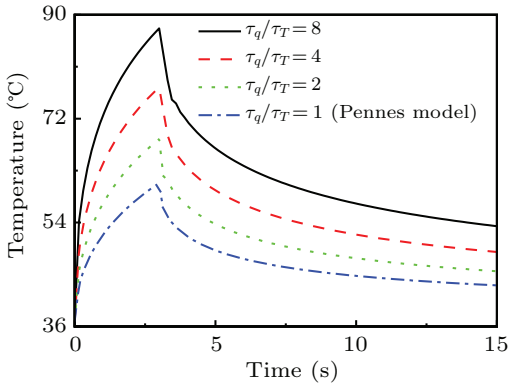


Fig. 4. Plots of time-dependent temperature response at pulsed heat flux surface with temperature-dependent properties for different values of ratio τ_q/τ_T.

Figure 4 displays the time-dependent temperatures in pulsed heat flux surface $x=0$ for different values of ratio τ_q/τ_T and given empirical value $a_1=0.0005$. It is obvious that the larger the ratio τ_q/τ_T, the higher the predicted temperature will be. The reason for such a phenomenon is attributed to the delay effect caused by thermal inertia, which is enhanced by controlling the value of the phase lag τ_q. With the phase lag τ_T increasing, the micro-structure effect strengthens and the wave-like behavior of heat transport is limited, then the temperature profiles decrease significantly.

Figure 5 further compares the history of temperature located in pulsed heat surface $x=0$ with temperature-dependent and constant thermal properties. The temperature elevations in tissue involving temperature-dependent thermal properties are found to be lower than those of the constant thermal properties. The difference between these two cases caused by both sides of the peak temperature, and it decreases significantly after the heat pulse has disappeared. Furthermore, the difference in temperature elevation induced by the temperature dependency of thermal properties also decreases with the ratio τ_q/τ_T decreasing. This means that the effect on the contributions of temperature-dependent thermal properties is opposite for two phase lags: the former is enhanced but the latter is weakened.

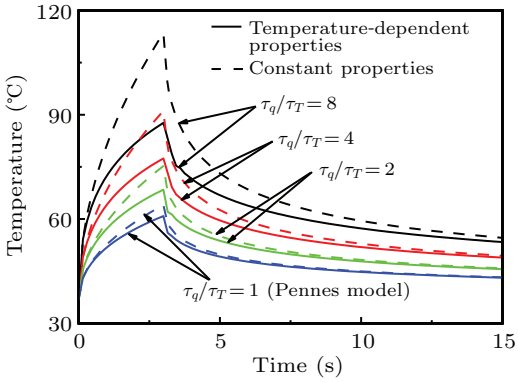


Fig. 5. Plots of time dependent temperature response at pulsed heat flux surface with temperature-dependent and constant thermal properties for different values of ratio τ_q/τ_T.

Figure 6 displays the temperature profiles varying with tissue depth with different times: $t=1.5$ s, 7.5 s, and 10 s, and given empirical value $a_1=0.0005$. Obviously, the wave-

like transport properties can be predicted for the delay effect. The thermal response region grows with heat transport and the temperature profile decreases significantly . Since the wave-like behavior is dominated by the phase lag τ_q, the delay effect is more significant for the case with a larger value of τ_q or τ_q/τ_T, which leads to a higher temperature gradient and a smaller thermal response region. Comparing with the constant property case, depicted in Fig. 7, the difference in temperature profiles focuses on the region near the pulsed heat flux surface, and this difference is not clear, can even be ignored for continuous heat transport.

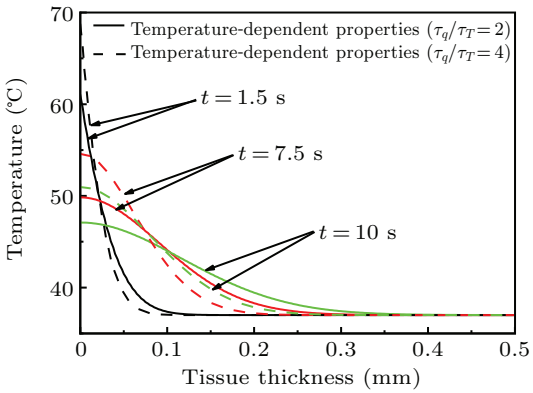


Fig. 6. Temperature distributions varying with tissue depth with temperature-dependent properties for different values of time t.

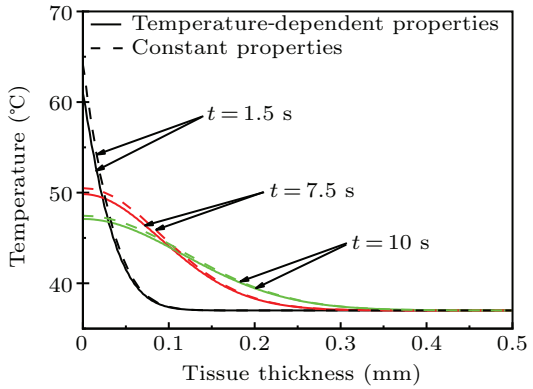


Fig. 7. Temperature distributions varying with tissue depth with temperature-dependent and constant thermal properties for different values of time t.

As discussed in the work of Guntur and Choi.[26], the overestimation of temperature with constant properties results from ignoring the contribution of temperature-dependent thermal properties. Based on Eq. (1), temperature gradient with respect to the time $\partial T/\partial t$ depends on thermal parameters k and c, in which the opposite contributions of parameters k and c can be observed clearly from the terms $\frac{k}{\rho c}\nabla^2 T$ and $\frac{1}{c}\frac{(q_{\rm met}+q_{\rm ext})}{\rho}$. With the increase of parameters c and k in the heating process, the rise of temperature induced by temperature dependent $k/\rho c$ is inessential comparing with the temperature decline induced by the temperature-dependent c in the heat source term. Consequently, the lower temperature can be predicted by using the temperature-dependent properties. Considering that the exterior heat input dominates the heat conduction happening in a short duration, the effects of temperature dependency on heat transport with different boundary pulsed heat fluxes are depicted in Fig. 8. It is seen clearly that the contribution of the specific heat c is further enhanced as the amplitude of pulsed heat flux q_0 increases, but that of the thermal conductivity k or $k/\rho c$ is opposite. As a result, the difference in temperature elevation between the two cases increases.

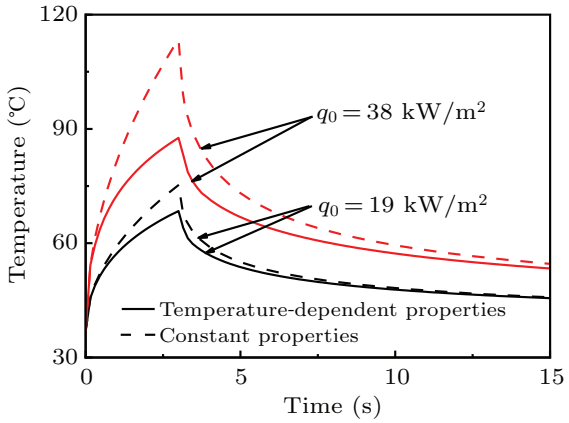


Fig. 8. Time dependent temperature responses at different pulsed heat flux surfaces with temperature-dependent and constant properties.

5. Conclusions and perspectives

The heat transport properties in living biological tissues with temperature-dependent properties are explored in the present work. An analytical procedure to deal with variable thermal parameters in the context of DPL model of bio-heat transfer is proposed. The thermal response of a skin tissue exposed to a pulsed heat flux, which frequently happens in heat therapies, is analyzed and some conditions can be drawn as follows.

(i) A lower temperature can be predicted by temperature-dependent properties when the skin tissueis heated, which is closer to the experimental observation than that predicted by the case with constant thermal properties.

(ii) The contributions of key temperature-dependent parameters k and c are opposite, and the contribution of parameter c is dominated for the heat conduction in a short time.

(iii) The effect of temperature dependency on heat transport is dependent on the vales of phase lag and the amplitude of the exterior pulsed heat flux. The difference in temperature predicted in the two cases is proportional to the ratio τ_q/τ_T and amplitude q_0.

(iv) The main difference in temperature induced by variable thermal properties focuses on the region near the pulsed heat flux surface, in which a lower temperature can be predicted. This means we should consider this temperature drop prior to selecting thermal dose in heat therapies.

Acknowledgement

Project supported by the National Science Foundation of China (Grant Nos. 51676086 and 51575247).

References

[1] Liu K C and Chen T M 2021 *J. Therm. Biol.* **98** 102907
[2] Anderozzi A, Brunese L, Iasiello M and Tucci C 2019 *Ann. Biomed. Eng.* **47** 676
[3] Matrin N A and Falder S 2017 *Burn* **43** 1624
[4] Sahoo N, Ghosh S, Narasimhan A and Das S K 2014 *Int. J. Therm. Sci.* **76** 208
[5] Xu F, Lu T J and Seffen K A 2008 *J. Mech. Phys. Solids* **56** 1852
[6] Xu F, Seffen K A and Lu T J 2008 *Int. J. Heat Mass Tran.* **51** 2237
[7] Pennes H H 1948 *J. Appl. Physiol.* **1** 93
[8] Roemer R B, Oleson J R and Cetas T C 1985 *American Journal of Physiology* **249** R153
[9] Mitra K, Kumar S, Vedavarz A and Moallemi M K 1995 *J. Heat Trans-T ASME* **117** 568
[10] Cattaneo C 1958 *Compte Rendus* **247** 431
[11] Vernotte P 1958 *Compte Rendus* **246** 3154
[12] Tzou T Y 1995 *J. Heat Trans. T. ASME* **117** 8
[13] Zhang Y W 2009 *Int. J. Heat Mass Tran.* **52** 4829
[14] Lin S M and Li C Y 2016 *Int. J. Therm. Sci.* **110** 146
[15] Liu K C 2015 *Int. J. Heat. Mass Tran.* **81** 347
[16] Liu K C, Wang Y and Chen Y 2010 *Int. J. Therm. Sci.* **49** 1138
[17] Liu J, Chen X and Xu L L 1999 *IEEE T. Bio-Med. Eng.* **46** 420
[18] Dutta J and Kundu B 2018 *Heat Mass Transfer* **54** 3199
[19] Liu K C and Chen Y S 2016 *Int. J. Therm. Sci.* **103** 1
[20] Liu K C and Chen H T 2015 *Int. Commun. Heat Mass* **65** 31
[21] Zhang Z W, Wang H and Qin Q H 2014 *J. Mech. Med. Biol.* **14** 1450060
[22] Kumar D, Singh S, Sharma N and Rai K N 2018 *Int. J. Therm. Sci.* **133** 320
[23] Arefmanesh A, Arani A A A and Emamifar A 2020 *Int. Commun. Heat Mass* **115** 104596
[24] Wang Y Z, Li M J and Liu D 2021 *Eur. J. Mech. A-Solid* **86** 104173
[25] Guntur S R, Lee K I, Paeng D G, Coleman A J and Choi M J 2013 *Ultrasound Med. Biol.* **39** 1771
[26] Guntur S R and Choi M J 2020 *Ultrasound Med. Biol.* **46** 1001
[27] Fu J W, Chen Z T and Qian L F 2015 *Compos. Struct.* **131** 139
[28] Balla M 1991 *Acta Mech.* **89** 73
[29] Wang Y Z, Zhang X B and Song X N 2012 *Acta Mech.* **223** 735
[30] Liang W, Huang S, Tan W S and Wang Y Z 2019 *Mech. Adv. Mater. Struct.* **26** 350
[31] Askarizadeh H and Ahmadikia H 2014 *Heat Mass Transfer* **50** 1673
[32] Askarizadeh H and Ahmadikia H 2015 *Appl. Math. Model.* **39** 3704
[33] Hobiny A D and Abbas I A 2020 *J. Therm. Stresses* **43** 1
[34] Wang Y Z, Zan C, Liu D and Zhou J Z 2019 *Eur. J. Mech. A-Solid* **76** 346